

**Ferumoxides - MR:**

**CT - CT**

1

2 . 3 . 4 . 5 .

ferumoxides - MR CT

(CTAP) - CT (CTHA)

: 20

CTAP - CTHA . MR

, T2\*

T1

30 . 20 160 28

가

receiver operating characteristic (ROC)

ROC (Az ) 가

statistic 가

: Az ferumoxides - MR 0.958, CTAP - CTHA 0.948

ferumoxides - MR

92.9%, CTAP - CTHA 90.9%

ferumoxides - MR 98.9%, CTAP - CTHA 93.6%

가

CTAP - CTHA

: Ferumoxides - MR CTAP - CTHA

(4, 5). CTAP - CTHA

(1)

(6 - 8), CT

. CT (CT during arterial portography,

CTAP ) (2, 3)

CT (CT hepatic arteriography, CTHA

)

CTAP - CTHA 가 가

Ferumoxides T2

Kupffer

MR

ferumoxides - MR

(9).

(10 - 17), ferumoxides -

MR (10, 13,

14, 16, 18 - 22).

1999

2000 10 19 2000 12 2



29 1 2  
 131 1 12 28  
 119  
 Ferumoxides - MR CTAP - CTHA  
 3  
 Caunaud (23)  
 3 가  
 가  
 umoxides - MR CTAP - CTHA fer -  
 2 가  
 5 , 4 , 가  
 2 , 3 , 1  
 Ferumoxides - MR CTAP - CTHA  
 maximum likelihood estimation binomial ROC  
 ROC

maximum likelihood curve fitting algorithm  
 ROC (24).  
 ROC (Az )  
 (25). two - tailed  
 Student t test p 0.05  
 가 가  
 3 2  
 ferumoxides - MR  
 CTAP - CTHA  
 McNemar test  
 p 0.05 가  
 Ferumoxides - MR CTAP -  
 CTHA 가  
 가 statistic ,  
 가 0.6 가 (26).  
 Ferumoxides - MR CTAP - CTHA  
 ROC maximum likelihood curve fit -  
 ting algorithm ROC Fig. 1  
 Ferumoxides - MR CTAP - CTHA  
 Az Table 1 . Az  
 ferumoxides - MR CTAP -  
 CTHA  
 Az (p > 0.05).  
 Ferumoxides - MR CTAP - CTHA

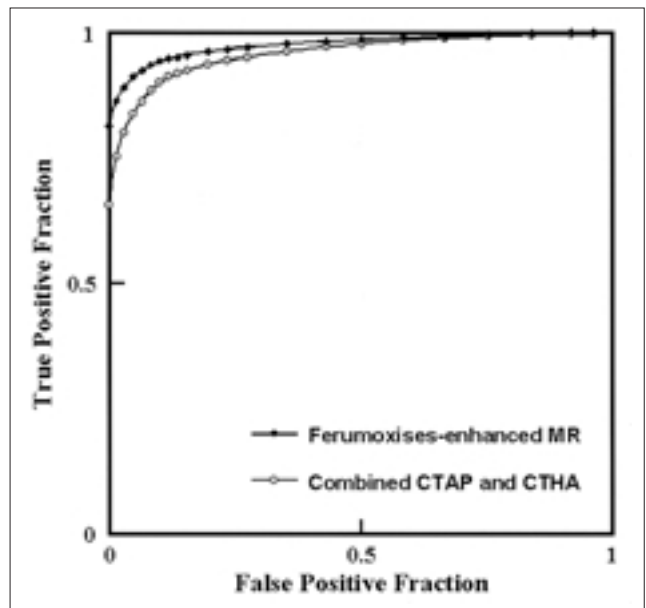


Fig. 1. Graph shows composite receiver operating characteristic(ROC) curves for pooled data reviewed by three observers.

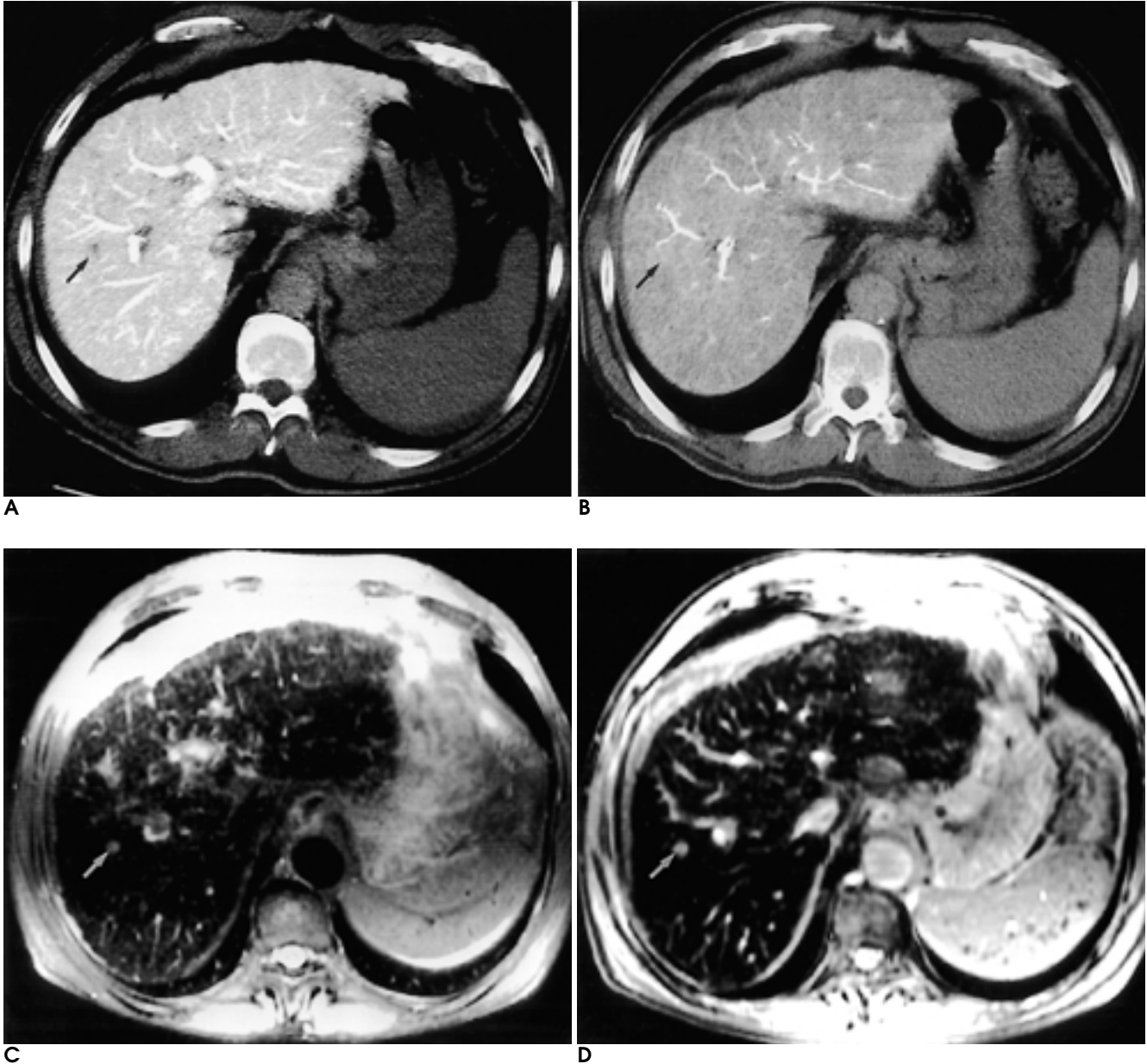
Table 2  
 fer -  
 umoxides - MR CTAP - CTHA  
 ferumoxides - MR  
 CTAP - CTHA  
 ferumoxides - MR 92.9%, CTAP - CTHA

Table 1. Area Under Curve (Az) values for HCC Detection in Ferumoxides-Enhanced MR and Combined CTAP and CTHA

	Az value		
	Ferumoxides-enhanced MR	Combined CTAP and CTHA	
Observer 1	0.982 (0.018)	0.973 (0.022)	p=0.591
Observer 2	0.946 (0.030)	0.931 (0.034)	p=0.541
Observer 3	0.963 (0.025)	0.941 (0.031)	p=0.254
Mean	0.964 (0.014)	0.948 (0.017)	p=0.183

Note HCC = hepatocellular carcinoma, CTAP = CT during arterial portography, CTHA = CT hepatic arteriography. Numbers in parentheses represent standard deviation.

90.5% 가 ( $p > 0.05$ , McNemar test), ferumoxides - MR 98.9%, CTAP - CTHA 93.6% 가 ( $p < 0.01$ , McNemar test). 가 ferumoxides - MR 6, CTAP - CTHA 8 가 2 cm (Table 3). 가 1 cm 3 1 ferumoxides - CTAP - CTHA 22 MR 4, CTAP - CTHA Ferumoxides - MR



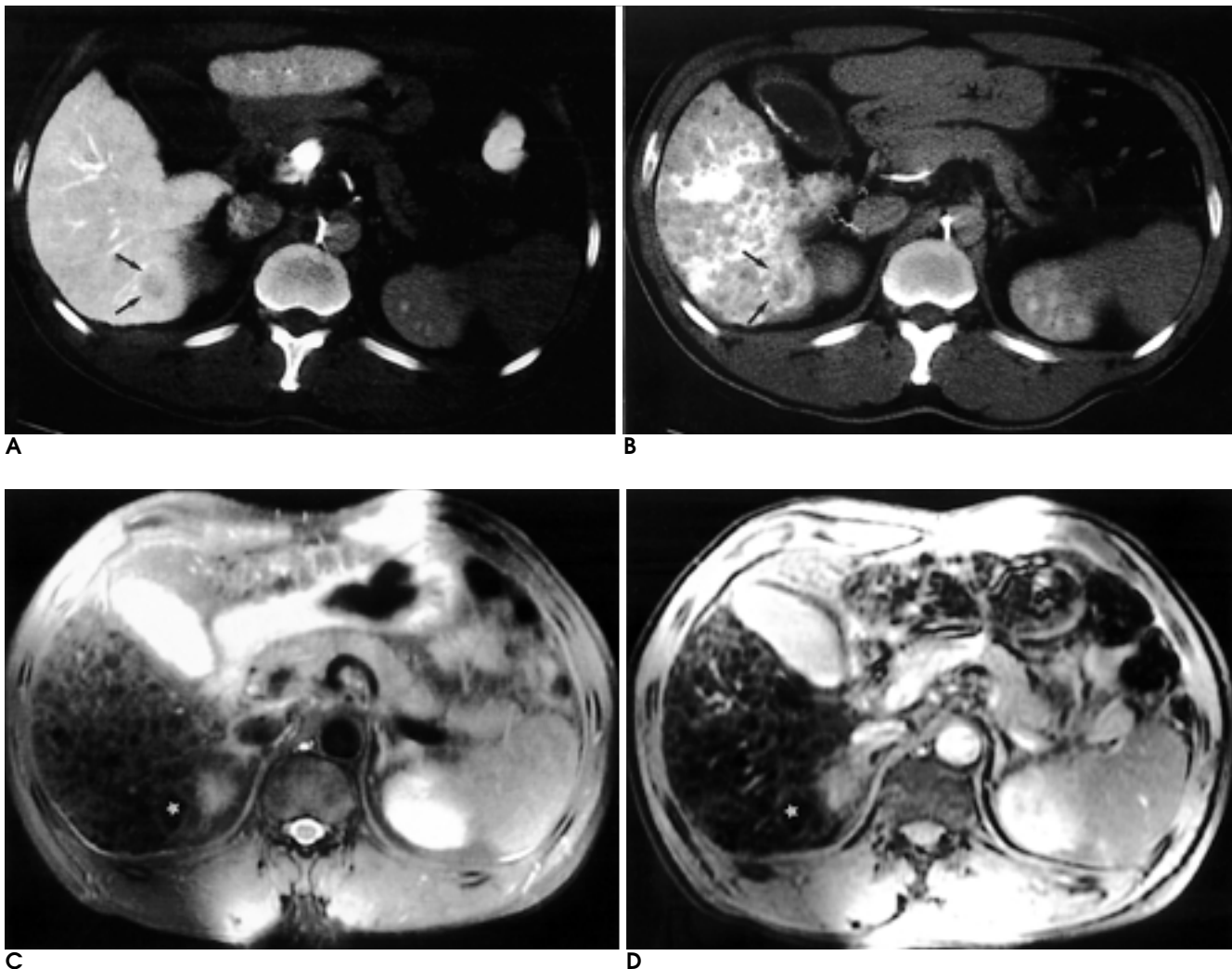
**Fig. 2.** 56-year-old man with 0.7 cm hepatocellular carcinoma in segment VIII.  
**A.** CT during arterial portography shows poorly defined small portal perfusion defect (arrow).  
**B.** CT hepatic arteriography shows subtle high attenuation (arrow) in the corresponding area of perfusion defect at CT during arterial portography.  
**C, D.** Ferumoxides-enhanced fat-suppressed respiratory-triggered fast spin-echo (TR = 5000 msec, TE = 18 msec) (**C**) and T2\*-weighted fast multiplanar gradient-recalled acquisition in the steady state (TR = 130 msec, TE = 8.4 msec, flip angle = 30°) (**D**) images demonstrate discrete high-signal intensity nodule (arrow).

4	1 cm (Fig. 4). CTAP - CTHA 22      19      (86%) (Fig. 5).	Ferumoxides -  (Table 4).	MR    CTAP - CTHA  0.06
---	---	---------------------------------	-------------------------------

**Table 2.** Relative Sensitivities and Specificities for HCC Detection in Ferumoxides-Enhanced MR and Combined CTAP and CTHA

	Ferumoxides-enhanced MR		Combined CTAP and CTHA	
	Sensitivity	Specificity	Sensitivity	Specificity
Observer 1	27/28 (96.4)	117/119 (98.3)	27/28 (96.4)	108/119 (90.1)
Observer 2	25/28 (89.3)	118/119 (99.2)	24/28 (85.7)	113/119 (95.0)
Observer 3	26/28 (92.9)	118/119 (99.2)	25/28 (89.3)	114/119 (95.8)
Total	78/84 (92.9)	353/357 (98.9)	76/84 (90.5)	335/357 (93.6)

Note HCC = hepatocellular carcinoma, CTAP = CT during arterial portography, CTHA = CT hepatic arteriography. Numbers in parentheses are percentage.

**Fig. 3.** 52-year-old man with 1.5 cm well differentiated hepatocellular carcinoma in segment VI.

**A.** CT during arterial portography shows oval portal perfusion defect(arrows).

**B.** Perfusion defect appears as area of low attenuation with irregular high attenuation rim(arrows) on CT hepatic arteriography. Note numerous tiny low attenuation lesions, all of which were proved as regenerative nodules histologically.

**C, D.** On ferumoxides-enhanced fat-suppressed respiratory-triggered fast spin-echo(TR = 4000 msec, TE = 18 msec) (**C**) and T2\*-weighted fast multiplanar gradient-recalled acquisition in the steady state(TR = 130 msec, TE = 8.4 msec, flip angle = 30°) (**D**), corresponding area shows low signal intensity(star), which can not be differentiated from adjacent regenerating nodules.

ferumoxides - MR (10 - 17).  
 ferumoxides - MR (11, 12, 18, 27) CTAP

**Table 3.** False-Negative Results of Ferumoxides-Enhanced MR and Combined CTAP and CTHA, According to HCC Size

Size of Largest HCC	Ferumoxides-enhanced MR			Combined CTAP and CTHA		
	Obs. 1	Obs. 2	Obs. 3	Obs. 1	Obs. 2	Obs. 3
1 cm (n = 3)	0	2	1	1	3	2
1 - 2 cm (n = 7)	1	1	1	0	1	1
2 cm (n = 18)	0	0	0	0	0	0

Note HCC = hepatocellular carcinoma, CTAP = CT during arterial portography, CTHA = CT hepatic arteriography, Obs. = observer. Data are number of segments containing hepatocellular carcinoma missed by observers.

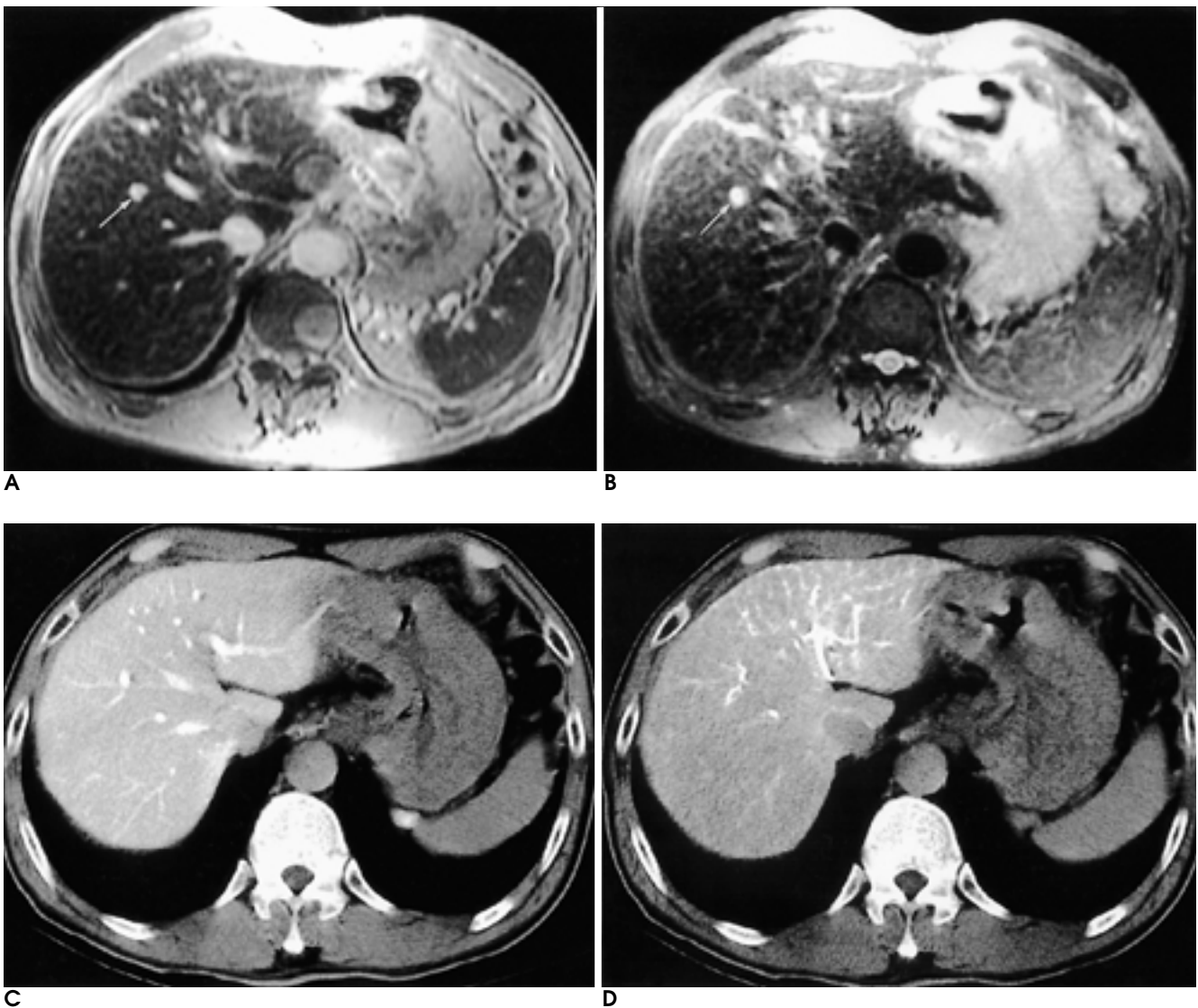


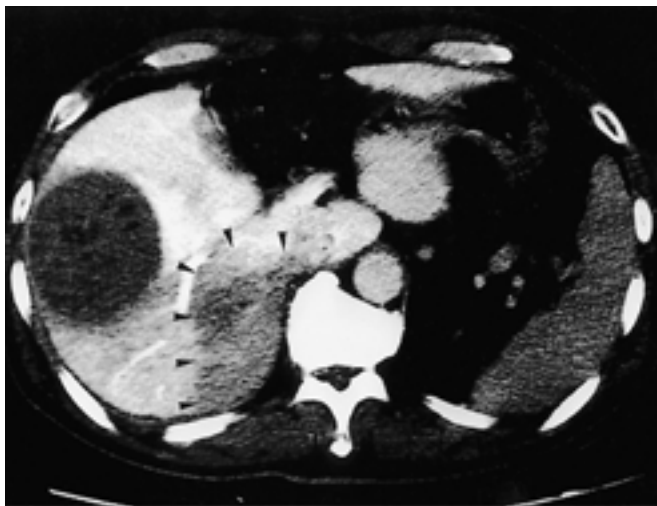
**Fig. 4.** 59-year-old man with 2.2 cm hepatocellular carcinoma in segment V (is not shown). **A, B.** Ferumoxides-enhanced fat-suppressed respiratory-triggered fast spin-echo (TR = 6000 msec, TE = 18 msec) (**A**) and T2\*-weighted fast multiplanar gradient-recalled acquisition in the steady state (TR = 130 msec, TE = 8.4 msec, flip angle = 30°) (**B**) show discrete small round high signal intensity nodule (arrow). Two observers interpreted this nodule as small hepatocellular carcinoma. **C, D.** There is no perfusion defect at CT during arterial portography (**C**) or high attenuation nodule at CT hepatic arteriography (**D**) in corresponding area. This false positive lesion at MR images is attributed to small vessel.

**Table 4.** Interobserver Agreement for HCC Detection in Ferumoxides-Enhanced MR and Combined CTAP and CTHA

	Ferumoxides-enhanced MR	Combined CTAP and CTHA
Observer 1 versus 2	0.955	0.771
Observer 1 versus 3	0.977	0.832
Observer 2 versus 3	0.978	0.809

Note HCC=hepatocellular carcinoma, CTAP=CT during arterial portography, CTHA=CT hepatic arteriography. Data are scores, which indicate the degree of agreement between two observers regarding the presence or absence of HCC in a segment.

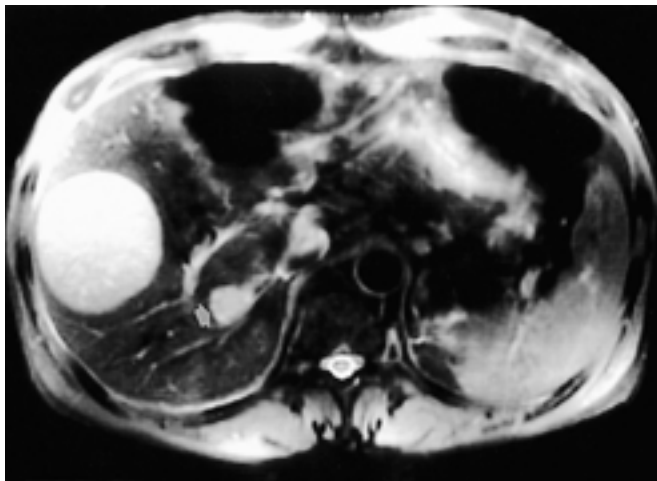
(15). 가 가 - MR CTAP-CTHA  
 가 (28, 29), ferumoxides - MR 가  
 - MR  
 가 - MR  
 (30) ferumoxides - MR  
 (17) 가  
 CTHA 가 가 CTAP-



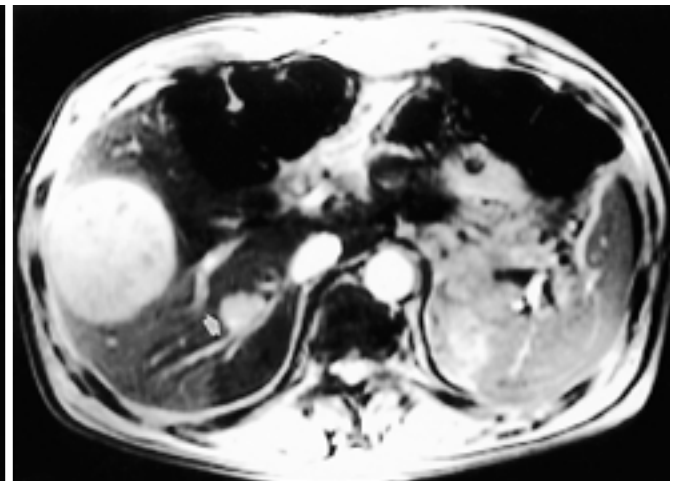
A



B



C



D

**Fig. 5.** 48-year-old man with two hepatocellular carcinomas measuring 6.5 cm and 1.5 cm in segment V and VI.

**A.** CT during arterial portography shows 6.5 cm round portal perfusion defect in segment V. Note geographic low attenuation (arrowheads) in posteromedial aspect of right hepatic lobe.

**B.** Portal perfusion defect in segment V on CT during arterial portography shows low attenuation containing irregular high attenuation on CT hepatic arteriography. Heterogeneous high attenuation area (arrowheads) corresponds to geographic perfusion defect on CT during arterial portography.

**C, D.** On ferumoxides-enhanced fat-suppressed respiratory-triggered fast spin-echo (TR = 6000 msec, TE = 18 msec) (**C**) and proton density-weighted fast multiplanar spoiled gradient-recalled echo (TR = 130 msec, TE = 8.4 msec, flip angle = 30°) (**D**), segment V mass show high signal intensity. Note another 1.5 cm high signal intensity nodule (arrow) in segment IV, which is uncertain on CT during arterial portography and CT hepatic arteriography.

CTAP가 (2, 3, 29) 8). (6- 84) : Ferumoxides - MR

가 가 . 160

76

MR

MR ferumoxides - MR

CTAP 43% (31). CTHA (36).

가 , (Fig. 5).

MR

CT CTAP - CTHA (14%, n=4)

CTAP - CTHA

CT 가

(32). CTAP CTHA 2 cm 가

(36%, n=10).

ferumoxides - MR

CTAP - CTHA

CTAP - CTHA 가 CTAP - CTHA

ferumoxides - MR

92.9%, CTAP - CTHA 90.5% 가

ferumoxides - MR

78 - 92% (13, 30), CTAP - CTHA

89 - 95% (4, 5).

ferumoxides - MR CTAP - 가

CTHA ferumoxides - MR

CTHA가 CTAP

ferumoxides - MR MR 가 가

ferumoxides - MR 가

T2 (10, 14, 33).

가

ferumoxides (18, 34, 35).

ferumoxides -

MR (13, 16, 21, 22, 27, 30),

(21, 36). T2\*

1. Malt RA. Current concepts: surgery of hepatic neoplasms. *N Engl J Med* 1985;313:1591-1595
2. Heiken JP, Weyman PJ, Lee JKT, et al. Detection of focal hepatic masses: prospective evaluation with CT, delayed CT, CT during arterial portography, and MR imaging. *Radiology* 1989;171:47-51
3. Nelson RC, Chezmar JL, Sugarbaker PH, Bernardino ME. Hepatic tumors: comparison of CT during arterial portography, delayed CT, and MR imaging for preoperative evaluation. *Radiology* 1989;172:27-34
4. Kanematsu M, Hoshi H, Imaeda T, Murakami T, Inaba Y, Nakamura H. Detection and characterization of hepatic tumors: value of combined helical CT hepatic arteriography and CT during arterial portography. *AJR Am J Roentgenol* 1997;168:1193-1198
5. Murakami T, Oi H, Hori M, et al. Helical CT during arterial portography and hepatic arteriography for detecting hypervascular hepatocellular carcinoma. *AJR Am J Roentgenol* 1997;169:131-135
6. Peterson MS, Baron RL, Dodd GD III, et al. Hepatic parenchymal perfusion defects detected with CTAP: imaging-pathologic correlation. *Radiology* 1992;185:149-155
7. Soyer P, Lacheheb D, Levesque M. False-positive CT portography: correlation with pathologic findings. *AJR Am J Roentgenol* 1993;160:285-289
8. Bluemke DA, Soyer P, Fishman EK. Nontumorous low-attenuation defects in the liver on helical CT during arterial portography: frequency, location, and appearance. *AJR Am J Roentgenol* 1995;164:1141-1145
9. Clement O, Siauve N, Cuenod C-A, Frija G. Liver imaging with ferumoxides (Feridex): fundamentals, controversies, and practical aspects. *Top Magn Reson Imaging* 1998;9:167-182
10. Winter TC III, Freeny PC, Nghiem HV, et al. MR imaging with IV superparamagnetic iron oxide: efficacy in the detection of focal hepatic lesions. *AJR Am J Roentgenol* 1993;161:1191-1198

11. Bellin MF, Zaim S, Auberton E, Sarfati G, Duron JJ, Khayat D, Grellet J. Liver metastases: safety and efficacy of detection with superparamagnetic iron oxide in MR imaging. *Radiology* 1994;193:657-663
12. Hagspiel KD, Neidl KF, Eichenberger AC, Weder W, Marincek B. Detection of liver metastases: comparison of superparamagnetic iron oxide-enhanced and unenhanced MR imaging at 1.5 T with dynamic CT, intraoperative US, and percutaneous US. *Radiology* 1995;196:471-478
13. Yamamoto H, Yamashita Y, Yoshimatsu S, et al. Hepatocellular carcinoma in cirrhotic livers: detection with unenhanced and iron oxide-enhanced MR imaging. *Radiology* 1995;195:106-112
14. Ros PR, Freeny PC, Harms SE, et al. Hepatic MR imaging with ferumoxides: a multicenter clinical trial of the safety and efficacy in the detection of focal hepatic lesions. *Radiology* 1995;196:481-488
15. Seneterre E, Taourel P, Bouvier Y, et al. Detection of hepatic metastases: ferumoxides-enhanced MR imaging versus unenhanced MR imaging and CT during arterial portography. *Radiology* 1996;200:785-792
16. Oudkerk M, van den Heuvel AG, Wielopolski PA, Schmitz PIM, Borel Rinkes IHM, Wiggers T. Hepatic lesions: detection with ferumoxides-enhanced T1-weighted MR imaging. *Radiology* 1997;203:449-456
17. *Comparison of Gad-DTPA and SPIO in the Detection of Liver Metastases*. *Radiology* 2000;42:265-272
18. Fretz CJ, Elizondo G, Weissleder R, Hahn PF, Stark DD, Ferrucci JT. Superparamagnetic iron oxide-enhanced MR imaging: pulse sequence optimization for detection of liver cancer. *Radiology* 1989;172:393-397
19. Schwartz LH, Seltzer SE, Tempany CM, et al. Superparamagnetic iron oxide hepatic MR imaging: efficacy and safety using conventional and fast spin-echo pulse sequences. *J Magn Reson Imaging* 1995;5:566-570
20. Van Beers BE, Lacroix M, Jamart J, et al. Detection and segmental location of malignant hepatic tumors: comparison of ferumoxides-enhanced gradient-echo and T2-weighted spin-echo MR imaging. *AJR Am J Roentgenol* 1997;168:713-717
21. Ward J, Chen F, Guthrie JA, et al. Hepatic lesion detection after superparamagnetic iron oxide enhancement: comparison of five T2-weighted sequences at 1.0 T by using alternative-free response receiver operating characteristic analysis. *Radiology* 2000;214:159-166
22. *Comparison of SPIO and MR : MR*. *Radiology* 2000;42:787-796
23. Dodd GD III. An American's guide to Couinaud numbering system. *AJR Am J Roentgenol* 1993;161:574-575
24. Metz CE. ROC methodology in radiologic imaging. *Invest Radiol* 1986;21:720-723
25. Hanley JA, McNeil BJ. The meaning and use of the area under a receiver operating characteristic (ROC) curve. *Radiology* 1992;143:29-36
26. Landis JR, Koch GG. The measurement of observer agreement for categorical data. *Biometrics* 1977;33:150-174
27. Ward J, Naik KS, Guthrie JA, Wilson D, Robinson PJ. Hepatic lesion detection: comparison of MR imaging after the administration of superparamagnetic iron oxide with dual-phase CT by using alternative-free response receiver operating characteristic analysis. *Radiology* 1999;210:459-466
28. Kanematsu M, Hoshi H, Murakami T, et al. Detection of hepatocellular carcinoma in patients with cirrhosis: MR imaging versus angiographically assisted helical CT. *AJR Am J Roentgenol* 1997;169:1507-1515
29. Hori M, Murakami T, Oi H, et al. Sensitivity in detection of hypervascular hepatocellular carcinoma by helical CT with intra-arterial injection of contrast medium, and by helical CT and MR imaging with intravenous injection of contrast medium. *Acta Radiol* 1998;39:144-151
30. Tang Y, Yamashita Y, Arakawa A, et al. Detection of hepatocellular carcinoma arising in cirrhotic livers: comparison of gadolinium- and ferumoxides-enhanced MR imaging. *AJR Am J Roentgenol* 1999;172:1547-1554
31. Oliver JH III, Baron RL, Dodd GD III, Peterson MS, Carr BI. Does advanced cirrhosis with portosystemic shunting affect the value of CT arterial portography in the evaluation of the liver? *AJR Am J Roentgenol* 1995;164:333-337
32. Jang H-J, Lim JH, Lee SJ, Park CK, Park HS, Do YS. Hepatocellular carcinoma: are combined CT during arterial portography and CT hepatic arteriography in addition to triple-phase helical CT all necessary for preoperative evaluation? *Radiology* 2000;215:373-380
33. Weissleder R. Liver MR imaging with iron oxides: toward consensus and clinical practice (editorial). *Radiology* 1994;193:593-595
34. Gillis P, Koeing SH. Transverse relaxation of solvent protons induced by magnetized spheres: application to ferritin, erythrocytes, and magnetite. *Magn Reson Med* 1987;5:323-345
35. Josephson L, Lewis J, Jacob P, Hahn PF, Stark DD. The effects of iron oxides on proton relaxivity. *Magn Reson Imaging* 1988;6:647-653
36. Soyer P. Will ferumoxides-enhanced MR imaging replace CT during arterial portography in the detection of hepatic metastases? Prologue to a promising future. *Radiology* 1996;201:610-611

## Ferumoxides -enhanced MR in the Detection of Hepatocellular Carcinoma: Comparison with Combined CT During Arterial Portography and CT Hepatic Arteriography<sup>1</sup>

Yoong Ki Jeong, M.D., Seung Hoon Kim, M.D.<sup>2</sup>, Jong Hwa Lee, M.D., Jae Cheol Hwang, M.D.,  
Soo Youn Ham, M.D., Neung Hwa Park, M.D.<sup>3</sup>, Chang Woo Nam, M.D.<sup>4</sup>,  
Jae Hee Seo, M.D.<sup>5</sup>, Seoung-Oh Yang, M.D.

<sup>1</sup>Department of Radiology, Ulsan University Hospital, University of Ulsan College of Medicine

<sup>2</sup>Department of Radiology, Samsung Medical Center, Sungkyunkwan University School of Medicine

<sup>3</sup>Department of Gastroenterology, Ulsan University Hospital, University of Ulsan College of Medicine

<sup>4</sup>Department of General Surgery, Ulsan University Hospital, University of Ulsan College of Medicine

<sup>5</sup>Department of Diagnostic Pathology, Ulsan University Hospital, University of Ulsan College of Medicine

**Purpose:** To compare the diagnostic accuracy of ferumoxides-enhanced MR with that of combined CT during arterial portography (CTAP) and CT hepatic arteriography (CTHA) in the preoperative detection of hepatocellular carcinoma (HCC).

**Materials and Methods:** For preoperative evaluation, 20 patients with HCC underwent ferumoxides-enhanced MR and combined CTAP and CTHA. The MR protocol included fat-suppressed respiratory-triggered fast spin echo, T2\*-weighted fast multiplanar gradient-recalled acquisition in the steady state, proton density-weighted fast multiplanar spoiled gradient-recalled echo, and breath-hold in-phase T1-weighted fast multiplanar spoiled gradient-recalled echo. In all patients, laparotomy was performed. The presence or absence of HCC was confirmed by pathologic examination in the resected liver and by intraoperative ultrasonography of remaining liver, or by follow up. Images were reviewed by three radiologists working independently; regarding the presence or absence of HCC in each segment, each observer assigned one of five confidence levels. A receiver operating characteristic (ROC) curve was fitted to these confidence ratings, and the diagnostic accuracy of each modality was evaluated by calculating the Az value (area under the ROC curve) and compared with that of other modalities. The sensitivity and specificity of each modality in the detection of HCC were also calculated and compared, and using a  $\chi^2$  statistic, inter-observer agreement for each modality was assessed.

**Results:** In 28 of 160 liver segments, 30 HCCs were present. For ferumoxide-enhanced MR the mean Az value was 0.958, and for combined CTAP and CTHA this value was 0.948. The difference was not statistically significant. The mean sensitivities of ferumoxide-enhanced MR and combined CTAP and CTHA were 92.9% and 90.9%, respectively, the difference being statistically insignificant. The mean specificities of these modalities were, respectively, 98.9% and 93.6%. The difference was statistically significant. For both ferumoxide-enhanced MR and combined CTAP and CTHA, interobserver agreement was excellent.

**Conclusion:** In the preoperative detection of HCC, ferumoxide-enhanced MR imaging of the liver showed a diagnostic accuracy similar to that of combined CTAP and CTHA. Its specificity, however, was higher.

### Index words : Iron

Liver, MR

Liver, CT

Liver neoplasms

Magnetic resonance (MR), contrast enhancement